Organometallics **1991**, *10*, 1922–1928

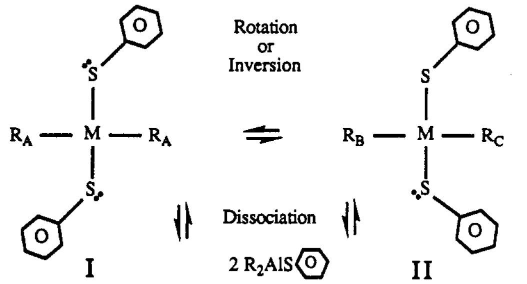

(2)

remain nonequivalent. Previous studies, on the cyclopropylaluminum system and on sulfur-bridged systems which have been found to be planar indicate that the conversion from the puckered configuration to planar should be a low-energy, rapid process. The rotation/inversion to convert I to II (eq 2) also must be rapid on the NMR time scale to lead to equivalence of the alkyl groups. The inversion barrier for sulfur bound to three centers is typically in the range 15–30 kcal/mol, and in the more complex system $[Me_2M(\mu\text{-}S\text{-}2,6Me_2C_6H_3)]_4$, the interconversion of ring conformations is slow on the NMR time scale with a barrier in excess of 25 kcal/mol.[15] These facts are inconsistent with inversion at sulfur. In contrast, we have established that the barrier to rotation of the cyclopropyl group in $[Me_2Al(\mu\text{-}C_3H_5)]_2$ is 11 kcal/mol[12] and that the barrier to rotation when oxygen is in the bridge varies widely depending on the substituent.[16] With C_6F_5 it is low, as noted earlier, giving rise to rapid rotation of the C_6F_5 group in **1a** and **2a**. We therefore conclude that the equivalence of the alkyl groups bound to the metal in $(R_2MSC_6F_5)_2$ results from two processes, flattening or rapid bending of the ring and rapid rotation of the $S\text{–}C_6F_5$ group about the C–S bond.

Acknowledgment is made to the donors of the Petroleum Research Fund, administered by the American Chemical Society, for the support of this research.

Supplementary Material Available: For **1a** and **2b** tables of anisotropic thermal parameters for the non-hydrogen atoms, atomic coordinates and isotropic thermal parameters for the hydrogen atoms, complete bond angles and distances, and least-squares planes and deviations and figures showing packing diagrams (23 pages); listings of observed and calculated structure factors (16 pages). Ordering information is given on any current masthead page.

---

[15] Bailey, M.; Barber, M.; Hendershot, D. G.; Kumar, R.; Oliver, J. P. Unpublished observations.

[16] Kumar, R.; Sierra, M. L.; de Mel, V. S. J.; Oliver, J. P. *Organometallics* **1990**, *9*, 484.

Structures of Organo-f-Element Compounds Differing in the Oxidation State of the Central Metal: Crystal Structures of Bis([8]annulene) Complexes of Cerium(IV), Ytterbium(III), and Uranium(III)

Thomas R. Boussie, David C. Eisenberg, John Rigsbee, Andrew Streitwieser,* and Alan Zalkin

Department of Chemistry, University of California, Berkeley, and the Lawrence Berkeley Laboratory, Berkeley, California 94720

Received October 1, 1990

Crystal structures of bis(methyl[8]annulene)cerium(IV) (**5**), [(diethylene glycol dimethyl ether)potassium] [bis([8]annulene)ytterbate(III)] (**14**), and [(diethylene glycol dimethyl ether)potassium] [bis(methyl[8]-annulene)uranate(III)] (**12**) are reported. These include the first structures of an organocerium(IV) compound and of a reduced uranocene. Crystals of **5** are orthorhombic, $P2_12_12_1$, with $a = 11.690$ (3) Å, $b = 14.315$ (3) Å, $c = 8.977$ (2) Å, $Z = 4$, and $R_F = 2.9\%$. Crystals of **14** are also orthorhombic, *Pbca*, with $a = 16.611$ (4) Å, $b = 14.219$ (5), Å, $c = 9.257$ (4) Å, $Z = 4$, and $R_F = 3.6\%$. Crystals of **12** are monoclinic, $P2_1/c$, with a = 13.833 (4) Å, $b = 9.989$ (3) Å, $c = 17.581$ (3) Å, $\beta = 95.87$ (3)°, $Z = 4$, and $R_F = 3.8\%$. These structures are compared to the previously reported structures of [(diethylene glycol dimethyl ether)potassium] [bis([8]annulene)cerate(III)] (**13**), bis[(dimethoxyethane)potassium] [bis([8]annulene)ytterbate(II)] (**15**), and uranocene (**1**). A comparison of the structural parameters of several additional [8]annulene metal complexes is also presented. The effect of coordination number on metal ligand distances in ionic complexes is discussed in terms of electrostatic interactions among the ligands.

Introduction

One of the most important factors affecting the structure and properties of an organometallic compound is the oxidation state of the central metal. In order to assess the effect of a change in oxidation state on the structural characteristics of a compound it is necessary to compare compounds in which there is little or no change in the coordinating ligands. However, the number of systems of this type for which structural information is available is quite limited, the principal examples thus far being the metallocenes. For example, in ferrocene[1] the metal–carbon distance is shorter than in the ferrocenium cation[2] despite the fact that the ionic radius of six-coordinate Fe(III) is generally smaller than that of six-coordinate Fe(II). A rationalization based on a covalent model suggests that

---

[1] (a) Dunitz, J. D.; Orgel, L. E.; Rich, A. *Acta Crystallogr.* **1956**, *9*, 373. (b) Seiler, P.; Dunitz, J. D. *Acta Crystallogr., Sect. B* **1979**, *35*, 1068.

[2] (a) Berstein, T.; Herbstein, F. H. *Acta Crystallogr., Sect. B* **1968**, *24*, 1640. (b) Bats, J. W.; DeBoer, J. J.; Bright, D. *Inorg. Chim. Acta* **1971**, *5*, 605.

Table I. Comparison of M–C Bond Lengths and r_{COT} for Several [8]Annulene Complexes

	compd	M C.N.	M[a] C.N.	M–C, Å	r_{metal}[b]	r_{COT}	ref
1	$U(C_8H_8)_2$	U^{4+}	10	2.647 (4)	1.08	1.57	5
2	$U(Me_4C_8H_4)_2$	U^{4+}	10	2.658 (4)	1.08	1.58	10
3	$U(C_8H_7SiMe_3)_2$	U^{4+}	10	2.659 (13)	1.08	1.58 (1)	21
4	$Th(C_8H_8)_2$	Th^{4+}	10	2.701 (4)	1.13	1.57	22
5	$Ce(MeC_8H_7)_2$	Ce^{4+}	10	2.692 (6)	1.07	1.62	
6	$(C_8H_8)UCl_2(NC_5H_5)_2$	U^{4+}	9	2.683 (6)	1.05	1.63	23
7	$(C_8H_8)U(acac)_2$	U^{4+}	9	2.694 (4)	1.05	1.64	23
8	$(C_8H_8)ThCl_2(thf)_2$[c]	Th^{4+}	9	2.72 (1)	1.09	1.63 (1)	24
				2.71 (2)	1.09	1.62 (2)	
				2.72 (2)	1.09	1.63 (2)	
9	$(C_8H_8)(C_5Me_5)Th(\mu\text{-}Cl)_2Mg(CH_2CMe_3)(thf)\cdot{}^1/_2(toluene)$[c]	Th^{4+}	10	2.739 (33)	1.13	1.61 (3)	25
				2.695 (33)	1.13	1.57 (3)	
10	$(C_8H_8)(C_5Me_5)Th[CH(SiMe_3)_2]$	Th^{4+}	9	2.746 (10)	1.09	1.66 (1)	25
11	$(C_8H_8)(C_5Me_5)Th[N(SiMe_3)_2]$	Th^{4+}	9	2.758 (12)	1.09	1.67 (1)	21
12	$[K(diglyme)][U(MeC_8H_7)_2]$[d]	U^{3+}	10	2.732 (8)	1.22	1.51	
		U^{3+}	10	2.707 (7)	1.22	1.49	
		K^+	8	3.263 (14)	1.51	1.75 (1)	
13	$[K(diglyme)][Ce(C_8H_8)_2]$[d]	Ce^{3+}	10	2.733 (4)	1.25	1.48	3
		Ce^{3+}	10	2.746 (6)	1.25	1.50	
		K^+	8	3.166 (17)	1.51	1.66 (2)	
14	$[K(diglyme)][Yb(C_8H_8)_2]$[d]	Yb^{3+}	10	2.610 (8)	1.10	1.51	
		Yb^{3+}	10	2.598 (4)	1.10	1.50	
		K^+	8	3.191 (4)	1.51	1.68 (1)	
15	$[K(glyme)]_2[Yb(C_8H_8)_2]$	Yb^{2+}	10	2.741 (10)	1.26	1.48 (1)	4
		K^+	7	3.017 (6)	1.46	1.56	
16	$(C_8H_8)Ti(C_5H_5)$	Ti^{3+}	8	2.323 (4)	0.77	1.55	26
17	$(C_8H_8)Ti(C_5Me_5)$	Ti^{3+}	8	2.34 (2)	0.77	1.57 (2)	27
18	$(C_8H_8)Zr(C_5Me_5)$[c]	Zr^{3+}	8	2.42 (2)	0.84	1.58 (2)	28
				2.474 (6)	0.84	1.63	
19	$(C_8H_8)Lu(C_5Me_5)$	Lu^{3+}	8	2.433 (1)	0.977	1.46	29
20	$(C_8H_8)ZrCl_2(thf)$	Zr^{3+}	8	2.458 (13)	0.84	1.62 (1)	30
21	$(C_8H_8)Lu(o\text{-}C_6H_4CH_2NMe_2)\cdot(OC_4H_8)$	Lu^{3+}	8	2.549 (15)	0.977	1.57 (1)	31
22	$[(C_8H_8)CeCl(thf)_2]_2$	Ce3+	9	2.710 (2)	1.20	1.51	32
23	$(C_8H_8)Yb(C_5H_5N)_3\cdot{}^1/_2(C_5H_5N)$	Yb^{2+}	8	2.64 (3)	1.14	1.50	33
24	$[K(diglyme)_2(Me_4C_8H_4)$	K^+	8	3.003 (8)	1.51	1.49	34
25	$K_2C_8H_8\cdot(OC_4H_8)_3$	K^+	8	2.943 (8)	1.51	1.43	35
26	$K_2C_8H_8\cdot(diglyme)$[d]	K^+	7	2.98 (2)	1.46	1.52 (2)	36
			7	3.05 (2)	1.46	1.59 (2)	

[a] See text for discussion of coordination number calculation. [b] From the tables of Shannon.[37] For coordination numbers for which ionic radii are not known, values are obtained from linear interpolation from known coordination numbers. [c] The molecule adopts more than one conformation in the crystal. [d] The [8]annulene rings are in different coordination environments.

oxidation of ferrocene removes an electron from a metal–ligand bonding orbital, resulting in an increase in the metal–carbon distance.

We have studied the effect of a change in oxidation state of the central metal on the structural parameters of bis([8]annulene)lanthanide and actinide complexes. While there exists theoretical[3] and experimental[4] evidence of covalency in these complexes, Raymond et al.[5] have pointed out that on the basis of crystal structure data for actinide, lanthanide, alkali-metal, and transition-metal [8]annulene complexes, there exists no direct *structural* evidence of metal–ligand covalent bonding. They found instead that the metal–ligand distance (but not necessarily other properties) could be rationalized by an ionic model based on the additivity of metal and ligand "radii". We have updated Raymond's analysis to include several newly published [8]annulene complexes (Table I), including the structures reported herein. These include the first structures of an organocerium(IV) compound and of a reduced uranocene.

A comparison of the structural parameters of f-element [8]annulene organometallic complexes differing in central metal oxidation state has features of particular interest. Accordingly, we report here the crystal structures of bis(methyl[8]annulene)cerium(IV) (5), [(diethylene glycol dimethyl ether)potassium] [bis([8]annulene)ytterbate(III)] (14), and [(diethylene glycol dimethyl ether)potassium] [bis(methyl[8]annulene)uranate(III)] (12) and compare the structural parameters of these compounds to previously published structures of bis([8]annulene) complexes of cerium(III),[6] ytterbium(II),[7] and uranium(IV).[8-10] Com-

---

(3) (a) Chang, A. H. H.; Pitzer, R. M. *J. Am. Chem. Soc.* **1989**, *111*, 2500. (b) Rösch, N. *Inorg. Chim. Acta* **1984**, *94*, 297. (c) Rösch, N.; Streitwieser, A. *J. Am. Chem. Soc.* **1983**, *105*, 7237. (d) Rösch, N.; Streitwieser, A. *J. Organomet. Chem.* **1978**, *145*, 195.

(4) (a) Brennan, J. G.; Green, J. C.; Redfern, C. M. *J. Am. Chem. Soc.* **1989**, *111*, 2374. (b) Streitwieser, A.; Kinsley, S. A.; Rigsbee, J. T.; Fragalà, I. L.; Ciliberto, E.; Rösch, N. *J. Am. Chem. Soc.* **1985**, *107*, 641. (c) Clark, J. P.; Green, J. C. *J. Chem. Soc., Dalton Trans.* **1977**, 505. (d) Fragalà, I. L.; Condorelli, G.; Zanella, P.; Tondello, E. *J. Organomet. Chem.* **1976**, *122*, 357. (e) Clark, J. P.; Green, J. C. *J. Organomet. Chem.* **1976**, *122*, C14.

(5) (a) Baker, E. C.; Halstead, G. W.; Raymond, K. N. *Struct. Bonding* **1976**, *25*, 23. (b) Raymond, K. N.; Eigenbrot, C. W., Jr. *Acc. Chem. Res.* **1980**, *13*, 276.

(6) Hodgson, K. O.; Raymond, K. N. *Inorg. Chem.* **1972**, *11*, 3030.

(7) Kinsley, S. A.; Streitwieser, A.; Zalkin, A. *Organometallics* **1985**, *4*, 52.

(8) Zalkin, A.; Raymond, K. N. *J. Am. Chem. Soc.* **1969**, *91*, 5667.

(9) Hodgson, K. O.; Raymond, K. N. *Inorg. Chem.* **1973**, *12*, 450.

(10) Sattelberger, A. P. Personal communication.

(11) Avdeef, A.; Raymond, K. N.; Hodgson, K. O.; Zalkin, A. *Inorg. Chem.* **1972**, *11*, 1083.

(12) Boussie, T. R.; Moore, R. M., Jr.; Streitwieser, A.; Zalkin, A.; Brennan, J.; Smith, K. A. *Organometallics* **1990**, *9*, 2010–2016.

(13) Zalkin, A.; Templeton, D. H.; Le Vanda, C.; Streitwieser, A. *Inorg. Chem.* **1980**, *19*, 2560.

(14) (a) Gilbert, T. M.; Ryan, R. R.; Sattelberger, A. P. *Organometallics* **1989**, *8*, 857. (b) M–C distances from a personal communication.

(15) Kroon, P. A.; Helmholdt, R. B. *J. Organomet. Chem.* **1970**, *25*, 451.

(16) Kool, L. K.; Rausch, M. D.; Rogers, R. D. *J. Organomet. Chem.* **1985**, *297*, 289.

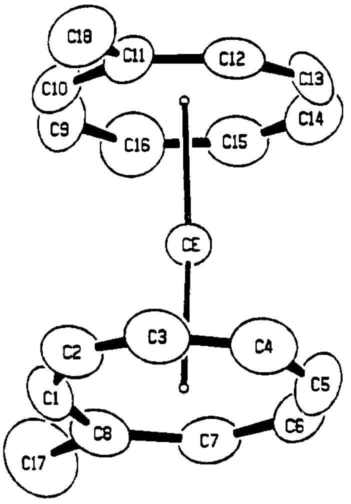

Figure 1. ORTEP diagram of 5.

pound numbers are those given in Table I.

Results and Discussion

Note on the Comparison of Structurally Related Compounds. We compare structures of bis[8]annulene complexes differing both in oxidation state of the central metal and in substitution of the [8]annulene rings, with the implicit assumption that substitution on the rings does not significantly affect the parameters we will be comparing, e.g. average metal–ligand bond distances. As evidence of this assumption, note that the structures of **2** and **3** are essentially the same as that of unsubstituted uranocene (**1**) with respect to metal–ring carbon distance and ring planarity. In the structures of all complexes containing substituted [8]annulene ligands (**2**, **3**, **5**, **12**, **24**) the ring C–C(R)–C is contracted from the normal value of 135 to 130–132° and the substituents are to differing degrees bent out of the plane. MNDO-optimized structures of the methylcyclooctatetraene dianion and the tetramethylcyclooctatetraene dianion reproduce these ring C–C(CH$_3$)–C angle contractions; presumably they arise from enhanced steric interactions between the methyl group and adjacent ring hydrogens resulting from the rather large interior angle of the eight-membered ring. A reduction of the ring angle results in separating adajacent substituents. In the comparison of metal structures that follows, this angle contraction has only a small effect on the average M–C bond distances.

Table II. Crystallographic Summary and Data Processing for 5, 14, and 12

	5	14	12
a, Å[a]	11.690 (3)	16.611 (4)	13.833 (4)
b, Å	14.315 (3)	14.219 (4)	9.989 (3)
c, Å	8.977 (2)	9.257 (4)	17.581 (4)
β, deg			95.87 (3)
cryst syst	orthorhombic	orthorhombic	monoclinic
space group	$P2_12_12_1$	$Pbca$	$P2_1/c$
V, Å^3	1502.2	2186.4	2416.6
d(calc), g cm^{-3}	1.664	1.539	1.780
Z	4	4	4
temp, °C	23	23	22
empirical formula	$C_{18}H_{20}Ce$	$C_{22}H_{30}O_3KYb$	$C_{24}H_{34}O_3KU$
F(000)	744	1004	1252
fw	376.48	506.63	647.67
color	black	blue	red
cryst size, mm	0.12 × 0.20 × 0.14	0.18 × 0.21 × 0.25	0.20 × 0.25 × 0.26
abs coeff, cm^{-1}	30.63	44.56	65.59
abs corr range	1.68–1.95	1.74–2.52	2.71–4.30
$(\sin\theta)/\lambda$ min, max	0.06, 0.65	0.06, 0.65	0.15, 0.60
hkl limits, $\pm h \pm k \pm l$	0,15; 0,18; ±11	0,21; ±18; −12,0	±16; 0,11; ±20
2θ scan width, deg	$1.50 + 0.693 \tan\theta$	$1.30 + 0.693 \tan\theta$	$1.50 + 0.693 \tan\theta$
no. of stds	3	3	3
no. of rflctns between stds	250	250	200
stds corr range	0.97–1.02	0.98–1.04	0.97–1.06
no. of scan data	3755	5052	8544
no. of unique rflctns	3468	2628	4279
no. of non-zero wtd data	2794 ($F^2 > 2\sigma$)	2183 ($F^2 > 2\sigma$)	2209 ($F^2 > 2\sigma$)
p[b]	0.035	0.06	0.05
extinction k[c]	1.73×10^{-7}	1.48×10^{-7}	1.75×10^{-7}
max % extinction corr	19.5%	16.5%	16.5%
no. of paramrs	263	174	262
R (non-zero wtd data)[d]	0.029	0.036	0.038
R_w[e]	0.030	0.043	0.043
R (all data)	0.047	0.046	0.109
goodness of fit[f]	1.01	1.12	1.13
max shift/esd	0.006	0.006	0.003
max/min, diff map (e Å^{-3})	1.66/0.55	0.83/0.83	1.77/2.39

[a] Unit cell parameters were derived by a least-squares fit to the setting angles of the unresolved Mo Kα components of 19 reflections ($25 < 2\theta < 37$) for **1**, 43 reflections ($20 < 2\theta < 36$) for **3**, and 20 reflections ($22 < 2\theta < 33$) for **5**. [b] In the least squares, the assigned weight $w = 4F^2[\sigma^2(F^2) + (pF^2)^2]^{-1}$, where F^2 is the observed structure amplitude and p is an assigned value that adjusts the weighted residuals of the strong reflections to be comparable to the weak ones. [c] Simple extinction correction has the form $(F_{obs})_{corr} = (1 + kI)F_{obs}$, where I is the uncorrected intensity and F_{obs} is the observed scattering amplitude. [d] $R = \sum[|F_{obs}| - |F_{cal}|]/\sum|F_{obs}|$. [e] $R_w = \{\sum[w|F_{obs}| - |F_{cal}|]^2/\sum(wF_{obs}{}^2)\}^{1/2}$. [f] σ_1 = error in observation of unit weight $= \{\sum(w[|F_{obs}| - |F_{cal}|]^2)/(no - nv)\}^{1/2}$, where no is the number of observations and nv is the number of variables.

Comparison of the Structures of Bis(methyl[8]annulene)cerium(IV) (5) and [(Diethylene glycol dimethyl ether)potassium] [Bis([8]annulene)cerate(III)] (13). Greco[26] et al. have reported preliminary X-ray structure data that suggest that Ce(C$_8$H$_8$)$_2$ (cerocene) is isostructural with (C$_8$H$_8$)$_2$U (uranocene, **1**) and (C$_8$H$_8$)$_2$Th (thorocene, **4**); however, a fully solved structure has not been published. Repeated attempts at our hands to obtain crystals of unsubstituted cerocene for a single-crystal X-ray analysis have proven fruitless, but suitable crystals of 1,1′-dimethylcerocene (**5**) were isolated. The ORTEP diagram, of the molecular structure is presented in Figure 1, and selected distances and angles are summarized in Tables IV and V.

The structure of **5** shows several interesting features. As with all other metallocene complexes containing monosubstituted [8]annulene rings, the ring substituents are not fully staggered; the dihedral angle between the methyl groups in **5** is approximately 120°. Furthermore, the methyl groups both lie inside the ring plane with bending angles of 1.9 and 4.2°, respectively. This phenomenon was

---

(17) Rogers, R. D.; Teuben, J. H. *J. Organomet. Chem.* **1989**, *359*, 41.

(18) Schumann, H.; Kohn, R. D.; Reier, F.-W.; Dietrich, A.; Pickart, J. *Organometallics* **1989**, *8*, 1388.

(19) Brauer, D. J.; Kruger, C. *Inorg. Chem.* **1975**, *14*, 3053.

(20) Wayda, A. L.; Rogers, R. D. *Organometallics* **1985**, *4*, 1440.

(21) Hodgson, K. O.; Raymond, K. N. *Inorg. Chem.* **1972**, *11*, 171.

(22) Wayda, A. L.; Mukerji, I.; Dye, J. L. *Organometallics* **1987**, *6*, 1328.

(23) Goldberg, S. G.; Raymond, K. N.; Harmon, C. A.; Templeton, D. H. *J. Am. Chem. Soc.* **1974**, *96*, 1348.

(24) Hu, N.; Gong, L.; Jin, Z.; Chen, W. *J. Organomet. Chem.* **1988**, *352*, 61.

(25) Noordik, J. H.; van den Hark, T. E. M.; Mooij, J. J.; Klaassen, A. A. K. *Acta Crystallogr., Sect. B* **1974**, *30*, 833.

(26) Greco, A.; Cesca, S.; Bertolini, G. *J. Organomet. Chem.* **1976**, *113*, 321.

Table III. Positional Parameters

atom	x	y	z
		(a) Compound 5	
Ce	0.00726 (2)	0.02994 (2)	0.12506 (3)
C1	0.0138 (8)	0.0539 (4)	−0.1699 (5)
C2	0.0212 (7)	−0.0430 (4)	−0.1481 (7)
C3	0.0892 (6)	−0.1019 (5)	−0.0615 (8)
C4	0.1752 (6)	−0.0887 (5)	0.0444 (8)
C5	0.2318 (5)	−0.0114 (7)	0.1007 (10)
C6	0.2249 (5)	0.0854 (6)	0.0824 (9)
C7	0.1596 (6)	0.1440 (5)	−0.0086 (7)
C8	0.0702 (5)	0.1330 (4)	−0.1138 (9)
C9	−0.2106 (5)	0.0917 (6)	0.1468 (10)
C10	−0.2182 (4)	−0.0057 (6)	0.1391 (10)
C11	−0.1662 (5)	−0.0847 (5)	0.2075 (7)
C12	−0.0836 (5)	−0.0903 (6)	0.3211 (7)
C13	−0.0198 (5)	−0.0255 (8)	0.4075 (6)
C14	−0.0102 (8)	0.0725 (7)	0.4150 (6)
C15	−0.0649 (6)	0.1463 (7)	0.3424 (10)
C16	−0.1472 (6)	0.1550 (5)	0.2286 (9)
C17	0.0232 (10)	0.2247 (6)	−0.1754 (10)
C18	−0.2026 (6)	−0.1773 (6)	0.1438 (13)
		(b) Compound 14	
Yb	0.00992 (2)	$^{1}/_{4}$	0.12447 (3)
K	0.18141 (9)	$^{1}/_{4}$	0.50650 (15)
O1	0.24203 (27)	$^{1}/_{4}$	0.7904 (5)
O2	0.20094 (26)	0.838 (3)	0.6510 (4)
C1	0.0141 (3)	0.2010 (6)	−0.1478 (6)
C2	−0.0299 (4)	0.1313 (4)	−0.0768 (6)
C3	−0.0935 (4)	0.1309 (4)	0.0233 (6)
C4	−0.1288 (3)	0.2004 (5)	0.0931 (6)
C5	0.1656 (6)	$^{1}/_{4}$	0.1573 (12)
C6	0.1416 (3)	0.1628 (10)	0.1909 (10)
C7	0.0847 (8)	0.1232 (5)	0.2783 (12)
C8	0.0265 (6)	0.1586 (8)	0.3703 (10)
C9	0.0036 (5)	$^{1}/_{4}$	0.4083 (10)
C10	0.2882 (3)	0.1672 (5)	0.8072 (6)
C11	0.2341 (4)	0.0848 (4)	0.7924 (6)
C12	0.1499 (5)	0.0071 (5)	0.6269 (7)
		(c) Compound 12	
U	0.25530 (4)	0.12337 (5)	0.00889 (2)
K	0.26172 (19)	0.48195 (28)	0.18729 (15)
O1	0.0901 (6)	0.6018 (9)	0.2077 (4)
O2	0.2570 (6)	0.7528 (9)	0.2376 (4)
O3	0.4257 (6)	0.6425 (10)	0.1904 (5)
C1	0.1845 (9)	−0.1321 (15)	−0.0119 (6)
C2	0.1187 (8)	−0.0436 (14)	−0.0564 (7)
C3	0.1251 (10)	0.0554 (14)	−0.1106 (7)
C4	0.2011 (14)	0.1193 (17)	−0.1438 (6)
C5	0.3025 (14)	0.1010 (17)	−0.1373 (7)
C6	0.3669 (10)	0.0220 (19)	−0.0943 (9)
C7	0.3636 (10)	−0.0732 (18)	−0.0422 (8)
C8	0.2834 (13)	−0.1421 (16)	−0.0070 (7)
C9	0.2640 (13)	0.3960 (17)	0.0130 (6)
C10	0.1641 (12)	0.3582 (18)	0.0350 (8)
C11	0.1319 (9)	0.2711 (7)	0.0864 (9)
C12	0.1694 (14)	0.1893 (20)	0.1386 (11)
C13	0.2554 (22)	0.1438 (16)	0.1659 (9)
C14	0.3554 (22)	0.1788 (24)	0.1484 (11)
C15	0.3913 (9)	0.2664 (19)	0.0968 (10)
C16	0.3546 (11)	0.3511 (15)	0.0423 (8)
C17	0.1398 (12)	−0.2216 (19)	0.0429 (8)
C18	0.2602 (21)	0.4893 (19)	−0.0573 (10)
C19	−0.0035 (11)	0.5664 (18)	0.1709 (9)
C20	0.0878 (10)	0.7267 (14)	0.2467 (7)
C21	0.1845 (10)	0.7547 (16)	0.2899 (7)
C22	0.3492 (9)	0.7888 (14)	0.2728 (7)
C23	0.4201 (10)	0.7765 (16)	0.2132 (7)
C24	0.4969 (10)	0.6245 (18)	0.1388 (9)

observed in $[1,3,5,7\text{-}(CH_3)_4C_8H_4]_2U$[9] and was suggested[27] to indicate covalent ring–metal interactions. An unusual feature of the molecule is the nonlinear ring-centroid–metal–ring-centroid angle of 176°. Nonlinear angles have also been observed in bis[8]annulene complexes of Yb(II) (177°),[7,28] U(III) (176°) (vide infra), and U(IV).[10] Solid-state and gas-phase structures[29] of several alkaline-earth-metal and lanthanide bis(pentamethylcyclopentadienyl) metallocenes exhibit nonlinear ring-centroid–metal–ring-centroid angles; angles in these complexes are more significantly nonlinear, between 130 and 160°. The origin of this nonlinearity has been the subject of much recent discussion,[29,30] with particular focus on the relative covalent and electrostatic contributions to the energy lowering upon bending. There appear to be no obvious packing effects or ligand–ligand interactions to explain the unusual nonlinear arrangement of ligands in **5**, and this relatively small deviation from linearity may arise from intramolecular electronic effects such as van der Waals attraction. Nevertheless, bending of these highly ionic complexes by 4° is energetically insignificant relative to even long-range crystal-packing forces.

Table IV. Selected Distances (Å) for 5, 14, and 12

5		14		12	
Ce–Ct1	1.975	Yb–Ct1	1.843	U–Ct1	1.999
Ce–Ct2	1.971	Yb–Ct2	1.902	U–Ct2	2.045
Ce–C1	2.671 (5)	Yb–C1	2.616 (6)	U–C1	2.745 (14)
Ce–C2	2.671 (6)	Yb–C2	2.601 (5)	U–C2	2.689 (11)
Ce–C3	2.699 (6)	Yb–C3	2.588 (5)	U–C3	2.710 (12)
Ce–C4	2.695 (6)	Yb–C4	2.587 (5)	U–C4	2.713 (11)
Ce–C5	2.699 (7)	Yb–C5	2.603 (10)	U–C5	2.725 (12)
Ce–C6	2.692 (6)	Yb–C6	2.589 (7)	U–C6	2.697 (13)
Ce–C7	2.697 (6)	Yb–C7	2.614 (6)	U–C7	2.680 (14)
Ce–C8	2.705 (7)	Yb–C8	2.635 (6)	U–C8	2.699 (15)
Ce–C9	2.703 (6)	Yb–C9	2.630 (9)	U–C9	2.727 (17)
Ce–C10	2.688 (5)			U–C10	2.725 (14)
Ce–C11	2.711 (6)			U–C11	2.725 (13)
Ce–C12	2.682 (7)			U–C12	2.757 (15)
Ce–C13	2.676 (6)			U–C13	2.767 (15)
Ce–C14	2.681 (6)			U–C14	2.746 (13)
Ce–C15	2.700 (7)			U–C15	2.700 (7)
Ce–C16	2.707 (7)			U–C16	2.707 (7)
		K–Ct2	2.670	K–Ct2	2.717
		K–O1	2.814 (5)	K–O1	2.715 (9)
		K–O2	2.734 (4)	K–O2	2.849 (10)
				K–O3	2.774 (9)

Table VI lists some pertinent data for the compounds being compared. For the Ce(III) complex **13**, note that the Ce atom is not located midway between the two [8]annulene rings, but rather is shifted away from the ring coordinated by potassium. This difference in Ce–ring distance can be understood in simple Coulombic terms. One [8]annulene ring is coordinated only to the central cerium cation, while the other ring is electrostatistically attracted to both the cerium and potassium cations. Accordingly, the second ring need not be as close to cerium as the first ring in the net balance of electrostatic interactions. As would be expected from the trends in ionic radius, the average metal–ring distance in the Ce(IV) complex **5** is less than that of either metal–ring distance in the Ce(III) complex **13**.

Comparison of the Structure of [(Diethylene glycol dimethyl ether)potassium] [Bis([8]annulene)ytterbate(III)] (14) and Bis[(dimethoxyethane)potassium] [Bis([8]annulene)ytterbate(II)] (15). The ORTEP diagram of the molecular structure of **14** is presented in Figure

---

[27] Luke, W. D.; Streitwieser, A. *ACS Symp. Ser.* **1979**, No. 131, 93.

[28] Kinsley, S. A.; Streitwieser, A.; Zalkin, A. *Acta Crystallogr., Sect. C* **1979**, *35*, 1068.

[29] Williams, R. A.; Hanusa, T. P.; Huffman, J. C. *Organometallics* **1990**, *9*, 1128–1134 and references therein.

[30] (a) Green, J. C.; Hohl, D.; Rösch, N. *Organometallics* **1987**, *6*, 712–720. (b) Andersen, R. A.; Boncella, J. M.; Burns, C. J.; Green, J. C. *J. Chem. Soc., Chem. Commun.* **1986**, 405–406. (c) Ortiz, J. V.; Hoffmann, R. *Inorg. Chem.* **1985**, *24*, 2095–2104. (d) Guido, M.; Gigli, G. *J. Chem. Phys.* **1976**, *65*, 1397–1402.

Table V. Selected Angles (deg) for 5, 14, and 12

5		14		12	
Ct1–Ce–Ct2	176.03	Ct1–Yb–Ct2	179.88	Ct1–U–Ct2	176.07
		Yb–Ct2–K	177.07	U–Ct2–K	173.83
		Ct2–K–O1	163.34	Ct2–K–O1	118.60
		Ct2–K–O2	117.37	Ct2–K–O2	159.59
				Ct2–K–O3	114.57
		O1–K–O2	60.05 (9)	O1–K–O2	59.48 (25)
				O2–K–O3	59.31 (26)
		O2–K–O2	119.56 (17)	O1–K–O3	117.82 (28)
		K–O1–C10	107.3 (3)	K–O2–C21	104.6 (8)
				K–O2–C22	109.3 (7)
		K–O2–C11	119.3 (3)	K–O1–C19	126.4 (8)
		K–O2–C12	121.6 (4)	K–O1–C20	120.8 (7)
				K–O3–C24	119.3 (7)
				K–O3–C24	122.3 (8)

Table VI. M–C and K–C Distances (Å)

complex	metal and oxidn state	ave M–C dist	ave K–C dist
5	Ce(IV)	2.692 (6)	
13	Ce(III)	2.733 (3) 2.746 (6)	3.166 (17)
14	Yb(III)	2.598 (4) 2.610 (8)	3.191 (14)
15	Yb(II)	2.741 (10)	3.017 (6)
12	U(III)	2.707 (7) 2.732 (8)	3.263 (35)
1	U(IV)	2.647 (4)	

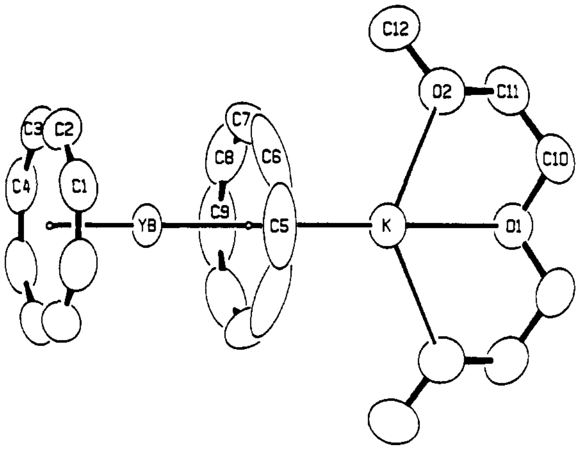

Figure 2. ORTEP diagram of **14**.

2 with selected distances and angles given in Tables IV and V. As in the example of **13** above, the Yb atom in **14** does not lie equidistant between the two rings, but rather has a shorter metal–ring carbon distance to the uncapped [8]annulene ring. The metal–ring carbon distances for both rings in **14** are smaller than the metal–ring carbon distance in **15** as a result of the smaller ionic radius of Yb(III) compared to Yb(II). The effect of changes in ionic radius is reflected also in a comparison of complexes **14** and **13**. The Yb–ring carbon distance in **14** is significantly smaller than the Ce–ring carbon distance in **13** as a result of the lanthanide contraction.

It is interesting to note that the K–ring carbon distance in **14** is much longer than that in **15**. The difference may arise from the better chelating capability of diglyme, which coordinates the potassium in **14**, over glyme, which coordinates the potassium atoms in **15**. An alternative explanation involves electrostatic interactions among ligands as discussed below.

Comparison of the Structures of [(Diethylene glycol dimethyl ether)potassium] [Bis(methyl[8]annulene)uranate(III)] (12) and Uranocene (1). As in the cerocene system discussed above, we were unable to obtain suitable X-ray-quality crystals of the unsubstituted U(III) complex while crystals of the 1,1′-dimethyl-substituted complex were isolable. The ORTEP diagram of the molecular structure of **12** is presented in Figure 3, and selected distances and angles are given in Tables IV and V.

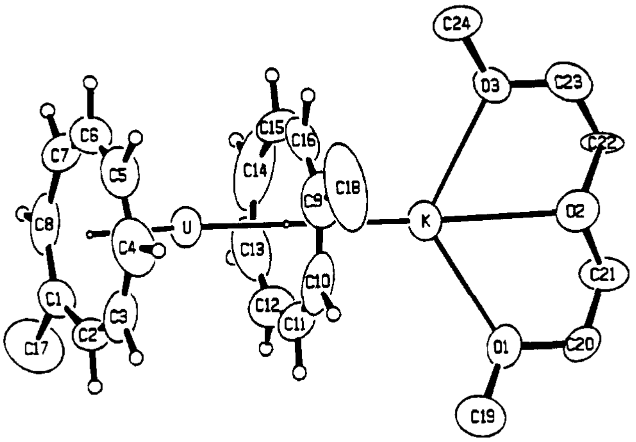

Figure 3. ORTEP diagram of **12**.

As in complexes **13** and **14**, **12** shows an asymmetrical displacement of the uranium atom between the two rings. And, as observed above, the U(IV)–ring carbon distance in **1** is less than the U(III)–ring carbon distance in **12**. The difference in metal–ring carbon distance in **12** and **1** is slightly smaller than in **14** and **15**, presumably because there is greater difference in ionic radius between the divalent and trivalent central metal than between the trivalent and tetravalent central metal.

As in **5** (discussed above), **12** exhibits a nonlinear ring-centroid–metal–ring-centroid angle (176°) and the methyl substituents in **12** are bent toward the uranium. The methyl on the ring uncomplexed by K (C17) is bent toward the U by 2.9°, while the opposite methyl (C16) is bent by 5.9°. The important point here is that organometallic compounds of U^{3+} are expected to have greater ionic character than those of U^{4+}. The fact that the methyl bending in **12** is comparable to that in **2** weakens the argument that such bending is indicative of ring–metal covalency.

Discussion of the Ionic Bonding Model. Raymond and Eigenbrot[5b] have used structural data to probe the degree of covalent bonding in structurally related metal complexes. By their method, an effective "ligand radius" is calculated by subtracting the metal ionic radius (corrected for charge and coordination number) from the metal–ligand distance. Through comparison of the ligand radii of various metal complexes one can directly assess the effect on structural parameters of a change in metal or metal oxidation state. In their analysis, both cyclopentadienyl and [8]annulene complexes were considered. Recently, Stockwell and Hanusa[31] updated Raymond's analysis of cyclopentadienyl complexes. They compiled an exhaustive survey of structural data of alkaline-earth-metal and f-element cyclopentadienyl compounds and performed a statistical analysis of the cyclopentadienyl ligand radii of these complexes. They cautioned against invoking covalency to rationalize the metal–ligand distances in f-element cyclopentadienyl complexes and pointed out the likely importance of steric interactions, particularly in the complexes of higher oxidation states.

Raymond and Eigenbrot similarly cautioned against inferring covalency from structural data, in both cyclopentadienyl and [8]annulene f-element complexes. They pointed out that an ionic model based on the additivity of metal cation and ligand anion radii was sufficient to rationalize the bonding in these complexes. In the 10 years since this argument was presented, structural analyses of several additional [8]annulene complexes have been obtained. We have updated Raymond and Eigenbrot's analysis to include these additional structures. Data from representative structures are summarized in Table I. The compounds in Table I do not represent all of the [8]annulene complexes for which structural data are known, just those whose coordination numbers are relatively unambiguous. Metal coordination numbers are calculated as the sum of electron pairs involved in interaction with the metal center. Thus, the cyclooctatetraene dianion is considered to contribute five to the coordination number count while cyclopentadienyl anion contributes three. Neutral coordinating ligands contribute one per coordinating heteroatom. Structures containing agostic interactions or fractional coordination numbers were omitted from Table I in order to facilitate direct comparison of structural parameters. In the following discussion, specific compounds are referred to by the number assigned to them in Table I.

There is significantly greater variation in the values of r_{COT} in the complexes listed in Table I than in those originally evaluated by Raymond and Eigenbrot. The range of values of r_{COT} derived from lanthanide and actinide metal–carbon distances in Table I is 1.46–1.67 Å. For the r_{COT} values derived from K–carbon distances, this range increases to 1.43–1.75 Å. The range of values of r_{COT} is quite large, but within roughly homologous compounds there is much closer agreement. For example, the bis([8]annulene)uranium(IV), -thorium(IV), and -cerium(IV) complexes 1 through 5 show values of r_{COT} in the range 1.57–1.62 Å. Similar agreement is evident in the structurally related compounds 6 through 8 (1.63–1.64 Å), 10 and 11 (1.66 and 1.67 Å), and 12 through 14 (1.48–1.51 Å). Greater variation is observed in the r_{COT} of related compounds 16 through 19 (1.46–1.63 Å). Despite the increase in range of r_{COT} values for these complexes, the differences are not easily ascribable to greater or lesser degrees of covalent bonding. In fact, examination of these data leads one to concur with Raymond and Eigenbrot's conclusion that there is no structural evidence for covalent bonding in these compounds. Moreover, recognition of the importance of ligand–ligand electrostatic repulsion allows rationalization of all significant variations in structural parameters for these compounds.

Comparison of the bis([8]annulene) complexes 1 and 3 with their mono([8]annulene) derivatives 6–8 is of interest. The ionic radius of nine-coordinate U(IV) is approximately 0.04 Å less than that of ten-coordinative U(IV),[32] and as the coordination number of the metal decreases from 10 in the bis([8]annulene) complexes to 9 in the mono([8]annulene) complexes, one would expect a shorter metal–carbon distance in the latter as a result of the smaller metal ionic radius. What is observed, however, is an increase in the metal–carbon distance on going from bis- to mono([8]annulene) complexes. This difference could be indicative of increased covalency in the uranocene-type compounds but other comparisons show that this argument is not compelling. For example, consider the K–C distances in compounds 12–14 and 24. In each case the coordination environments of the potassium atom are identical; a cyclooctatetraene dianion coordinates one side of the potassium ion, while a single diglyme coordinates the other side. One might then expect the K–C distances to be approximately the same. However, in each of the sandwich complexes the K–C distance is significantly greater than that in 24.

These observations can be rationalized by including effects of electrostatic interaction of more than just nearest neighbors. In an ionic model of 24 each potassium is attracted to the central dianion and is repelled by the other cation. In 12–14, however, the potassium is repelled by the more highly charged metal +3 cation, which also attracts the cyclooctatetraene dianion more strongly. Accordingly, the K^+–ring distances are greater in the latter compounds. Similarly, in the half-sandwich compounds 6–8 the metal–Cl and –O anion distances are less than the metal–ring distances and ring–ligand repulsions will be greater than the ring–ring repulsions in 1–4. Additional repulsions in the half-sandwich compounds of 6 and 8 come from the dipoles of coordinated pyridine and THF, respectively. The same effect is shown in reverse for the sandwich and dimeric half-sandwich compounds of Ce^{3+}, 13 and 22, respectively. Both ring–metal distances are greater in 13 than in 22 because the bridging chlorides in 22 are farther from each metal and repulsions to the cyclooctatetraene dianion rings are less than in the monomeric half-sandwich chlorides 6 and 8.

Steric effects between ligands would not appear to be significant in the bis([8]annulene) metallocenes. Within experimental error the M–C distances in compounds 1–3 are equal. The rings are approximately 4 Å apart, and ring substituents can adopt staggered conformations if necessary to avoid unfavorable steric interactions. In more sterically congested systems, ring–ligand interactions may be more pronounced. Comparison of ten-coordinated 4 with 9 (whose coordination environment, while formally ten-coordinate, is significantly different from 4) shows no significant difference in the cyclooctatetraene dianion C–Th distances. However, comparison of ten-coordinate 9 with the related nine-coordinate compounds 10 and 11 indicates the likelihood of significant steric interactions when extremely bulky ligands such as bis(trimethylsilyl)amido and bis(trimethylsilyl)methyl are utilized. Steric factors aside, the Th–C distances in nine-coordinate 10 and 11 would be expected to be shorter than those in ten-coordinate 4 and 9. That they are actually the same or slightly *longer* suggests that steric interactions are involved in 10 and 11.

Other structural effects can be rationalized in the same manner. For the two eight-coordinated Lu^{3+} compounds 19 and 21, 21 features a short bond to an aryl anion. The repulsion between this anion and the cyclooctatetraene dianion ring results in a substantially longer Lu–ring

---

[31] Stockwell, S. C.; Hanusa, T. P. *Inorg. Chem.* **1990**, *29*, 76–80.

[32] Shannon, R. D. *Acta Crystallogr., Sect. A* **1976**, *32*, 751.

distance than in **19**. In some cases both the coordination number and the electrostatic interactions among ligands lead to the same result. For example, in **23** the cyclooctatetraene dianion ring is repelled only by pyridine dipoles and the ring–metal distance is expected to be shorter than in **15** where the two dianion rings repel each other. But the Yb is ten-coordinated in **15** and only eight-coordinated in **23**, which leads to the same conclusion. Indeed, it seems likely that the effect of coordination number in such complexes, in which ionic bonding is dominating, result from simple Coulombic interactions among the ligands. That is, the higher effective ionic radius of more highly coordinated metal cations is not an intrinsic effect of the cation but is simply a result of increased Coulombic repulsions among the ligands.

Acknowledgment. This work was supported by the Director, Office of Energy Research, Office of Basic Energy Sciences, Chemical Sciences Division of the U.S. Department of Energy under Contract No. DE-AC03-76SF00098.

Experimental Section

Bis(methyl[8]annulene)cerium(IV)[33] (5). In an argon-filled glovebox illuminated with a red light, 0.20 g (0.48 mmol) of $KCe(CH_3C_8H_7)_2$[34] was dissolved in 30 mL of THF and to this pale green solution was added 1.17 g (5.0 mmol) of freshly ground AgI. The mixture was stirred for 2 min and filtered through very fine filter paper to yield a dark red filtrate and black precipitate. The THF was removed from the filtrate in vacuo, and the solid was recrystallized from hexane to afford 0.14 g (78%) of dark red crystals of **5**. ^1H NMR (THF-d_8, 30 °C): δ 2.01 (s, 3 H), 5.70 (m, 7 H). UV–vis (THF): 4.77 (s), 570 (w) nm. X-ray-quality crystals were obtained by slow cooling to −20 °C of a concentrated hexane solution of **5**.

[(Diethylene glycol dimethyl ether)potassium] [Bis([8]-annulene)ytterbate(III)][34] (14). Fresh-cut potassium metal (0.74 g, 19 mmol) was added to a solution of 0.92 g (8.88 mmol) of COT in 50 mL of THF and stirred for 3 h. The K_2COT solution was added dropwise to a rapidly stirred suspension of 1.23 g (4.40 mmol) of anhydrous $YbCl_3$ in 100 mL of THF, and the mixture was stirred for 2 h as the solution turned dark blue and a pink precipitate formed. The solution was filtered and concentrated, and to it was added 10 mL of diglyme. The product was recrystallized by liquid hexane diffusion into a THF/diglyme solution to afford 0.72 g (29%) of **14** as bright blue crystals. X-ray quality crystals were obtained from a second recrystallization.

[(Diethylene glycol dimethyl ether)potassium] [Bis(methyl[8]annulene)uranate(III)][35] (12). To a solution of THF (100 mL) and diglyme (10 mL) was added 1.0 g (2.11 mmol) of 1,1′-dimethyluranocene,[36] 0.01 g (0.1 mmol) of naphthalene, and 0.10 g (2.56 mmol) of fresh-cut potassium metal. The mixture was stirred for 2 h, while the color turned from dark green to brown. The solution was filtered and concentrated, and the flask was connected via a U-tube to a second flask containing 40 mL of pentane. After several days 0.75 g (55%) of reddish brown crystals of **12** were collected. ^1H NMR (THF-d_8, 35 °C): −5.2 (s, 40 Hz, 3 H), −29.3 (s, 200 Hz, 2 H), −29.9 (s, 200 Hz, 1 H), −32.7 (s, 200 Hz, 2 H), −35.3 (s, 200 Hz, 2 H). X-ray-quality crystals were obtained from this crop. This compound is extremely air sensitive.

X-ray Diffraction. The air-sensitive crystals were sealed inside quartz capillaries. A modified Picker FACS-I automated diffractometer equipped with a graphite monochromator and a Mo X-ray tube ($\lambda(K\alpha_1) = 0.70930$ Å) was used to collect sets of θ–2θ-scanned X-ray diffraction intensities; the experimental details are given in Table I. The metal atom positions were deduced from three-dimensional Patterson functions, and after least-squares refinement of the metal atoms, carbon and oxygen atoms were located from subsequent Fourier maps. The positional and anisotropic thermal parameters of all of the non-hydrogen atoms were adjusted with the use of a full-matrix least-squares refinement procedure. Hydrogen atom parameters were included with isotropic thermal parameters, but not all of them could be refined. In **14**, the hydrogen atom locations were estimated when they were not observed in the difference electron density maps and, with the exception of five hydrogen atoms (on the ring between the Yb and K atoms), were allowed to refine with no restrictions; the five hydrogen atoms were included with fixed atomic parameters and not refined. In **12**, all of the hydrogen atoms were included with fixed parameters and were not varied; some 55 low-angle data, whose $(\sin\theta)/\lambda < 0.15$, were all deleted from the U complex data set, as a few of them exhibited large discrepancies between the observed and calculated values which were attributed to an imperfect absorption correction on an irregularly shaped crystal. In **5** the positional parameters of the hydrogen atoms were refined with imposed distance restraints[37] (C–H 0.95 ± 0.02 Å, methyl H–H 1.51 ± 0.05 Å); isotropic thermal parameters were assigned to the hydrogen atoms globally for each ring and each methyl group. The results of the least-squares refinements are given in Table I. With the exception of ORTEP,[38] all computer programs are our own; scattering factors and anomalous dispersion terms were taken from ref 39. Thermal parameters, hydrogen positions, additional bond lengths and angles, least-squares planes, and structure factor tables are available as supplementary material.

Supplementary Material Available: Textual details of the crystal data and tables of thermal parameters, positional parameters, bond distances and angles, and least-squares planes (8 pages); listings of structure factors (20 pages). Ordering information is given on any current masthead page.

---

[33] (a) Rigsbee, J. T. Ph.D. Dissertation, University of California, Berkeley, 1988. (b) Streitwieser, A.; Kinsley, S. A. In *Fundamental and Technological Aspects of Organo-f-Element Chemistry*; Marks, T. J., Fragal, H. I. C., Eds.; D. Reidel: Dordrech, 1985; pp 77–114.

[34] For a general synthesis of this class of compound, see: Hodgson, K. O.; Mares, F.; Starks, D. F.; Streitwieser, A. *J. Am. Chem. Soc.* **1973**, *95*, 8650.

[35] For a more detailed discussion of this class of compound, see: Eisenberg, D. C.; Streitwieser, A.; Kot, W. K. *Inorg. Chem.* **1990**, *29*, 10.

[36] See Harmon, C. A.; Streitwieser, A. *Inorg. Chem.* **1973**, *12*, 1102 and references therein for syntheses of substituted uranocenes.

[37] Waser, J. *Acta Crystallogr.* **1963**, *16*, 1091.

[38] Johnson, C. K. Report ORNL-37945, 1965; Oak Ridge National Laboratory, Oak Ridge, TN.

[39] *International Tables for X-ray Crystallography*; Kynoch Press: Birmingham, England, 1974; Vol. IV.